

Preliminary performance measurements for a streak camera with a large-format direct-coupled charge-coupled device readout

R. A. Lerche,^{a)} J. W. McDonald, R. L. Griffith, G. Vergel de Dios, D. S. Andrews, A. W. Huey, P. M. Bell, and O. L. Landen

Lawrence Livermore National Laboratory, Box 808, Livermore, California 94551

P. A. Jaanimagi and R. Boni

University of Rochester Laboratory for Laser Energetics, 250 East River Road, Rochester, New York 14623

(Presented on 21 April 2004; published 12 October 2004)

The University of Rochester's Laboratory for Laser Energetics (Rochester, New York) is leading an effort to develop a modern, fully automated streak camera. Characterization of a prototype camera shows spatial resolution better than 20 lp/mm, temporal resolution of 12 ps, line-spread function of 40 μm (full width at half maximum) contrast transfer ratio of 60% at 10 lp/mm, system gain of 101 charge-coupled device electrons per photoelectron, and a dynamic range of 500 for a 2 ns window. © 2004 American Institute of Physics. [DOI: 10.1063/1.1788890]

I. INTRODUCTION

The Lawrence Livermore National Laboratory (LLNL) Laser Programs built ~30 high-speed compact optical streak cameras¹ in the 1970s and 1980s. These cameras have provided the Inertial Confinement Fusion (ICF) Program with high-speed recording capability for 30 years. The cameras record streak images for a variety of laser, x-ray, and particle instruments that require temporal resolutions ~10 ps. The cameras use an RCA C73435 streak tube directly coupled to a microchannel-plate (MCP) image-intensifier tube IIT. In 1987, charge-coupled device (CCD) readouts replaced original film packs on 15 cameras built for the Nova laser project. A lens relayed the IIT image to the CCD because direct fiber-optic (FO) coupling was not yet reliable.

Unfortunately, the cameras are difficult to maintain because components, including streak tube and IIT, are no longer available. Furthermore, the National Ignition Facility (NIF) projects a need for ~50 optical streak cameras. This article describes work related to the ICF Program's search for optical streak cameras whose performance is equal to or better than the original Livermore design.

The University of Rochester's Laboratory for Laser Energetics (Rochester, NY) (LLE) is leading an effort to develop a modern, totally automated streak camera. Their design incorporates years of experience using Livermore cameras and cameras of a more recent LLE design.² Performance requirements for the camera are driven by the needs of LLE's OMEGA Laser Facility. These are similar to the needs of the NIF. Performance of a prototype camera has been measured; preliminary results are reported in this article.

II. THE ROCHESTER OPTICAL STREAK SYSTEM

The streak camera characterized for this article is called the ROSS (Rochester Optical Streak System). Its Photonis

P-510 streak tube shares many similarities with the RCA C73435: a large format (40-mm diam), a slot-type extraction grid, 15-kV photocathode voltage, and similar internal electrode structures. Perhaps the most significant difference is the photocathode-to-extraction grid spacing (3.5 mm for the P-510, 7 mm for the C73435). For identical voltages, the higher electric field at the P-510 photocathode allows a higher linear current density to be extracted and reduces electron transit-time dispersion through the tube.

Streak tubes can have a slot- or a mesh-type extraction grid. Electrostatic lenses formed by the slot and the focus grid can focus electrons from a relatively wide strip (0.5 to 1 mm) on the photocathode to a narrow line at the tube's output. Because image width for a mesh-type tube is proportional to the width of the illuminated strip, its input slit is typically <100 μm wide to maintain good time resolution. Thus, a slot-type tube can have ten times more usable photocathode area, ten times more sensitivity, and support ten times more current than a mesh-type tube.

The ROSS does not use a MCP IIT. It has long been known that the IIT limits camera spatial resolution.³ The ROSS, like the earlier LLE camera, couples the streak tube image directly to a CCD through a coherent FO coupler. Low noise, improved efficiency, and high amplifier gain of modern CCDs and improved FO/CCD coupling now allow single photoelectrons to produce signals greater than the image noise without an IIT. The ROSS uses a Spectral Instrument SI-800 CCD camera with a 2K×2K E2V 42–40 back-illuminated CCD with 13.5 μm pixels and a 1:1 FO coupler.

The ROSS consists of a main streak camera module and an optics module. The camera module contains the streak tube, CCD, power supplies, and digital interface electronics; the optics module contains calibration light sources, slits, filters, and imaging optics for safely coupling optical signals into the streak tube. The camera module has been designed and a prototype built. Optics module design is nearing completion. All data acquired for this article used the slit and lens arrangement from a Livermore streak camera. The

^{a)}Electronic mail: lerche1@llnl.gov

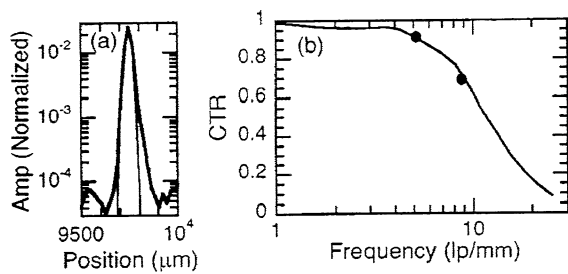


FIG. 1. Spatial resolution. (a) Line spread function and Gaussian with a 40- μm FWHM, (b) contrast transfer function (CTF). Circles are Ronchi ruling measurements.

ROSS prototype contained a P-510 tube with S-20 photocathode. The goal of this work was to understand the performance of the streak camera module, not the optics module.

III. STREAK CAMERA CHARACTERIZATION

Characterization determines how a camera performs for a variety of operating conditions. In this study, we evaluated (1) magnification, (2) spatial resolution, (3) temporal resolution, (4) noise, (5) gain, and (6) dynamic range. The camera was set up using techniques similar to those used with Livermore cameras. Unless noted otherwise, measurements used a 1-mm wide slit illuminated with a collimated 532-nm laser. Collimated light creates a large depth of field and eliminates the input optic as a factor in resolution measurements.

Spatial magnification and field of view (FOV) were measured with a mask of 10- μm slits evenly spaced 1.5 mm apart. The mask was placed in two different positions: against the streak tube input window to measure the tube's magnification and at the slit plane to measure the camera system magnification. Measured streak tube magnification of 1.35 matches the tube spec of 1.3. The input optics has an additional magnification of 1.16 giving the system a magnification of 1.57. All measurements in this article are referred to the streak tube photocathode. A single pixel at the CCD views 10 μm of the streak camera's photocathode. The camera's FOV is limited to 20.5 mm by the CCD which views a 27.6 mm square of the 60 mm diam image.

A line-spread function (LSF) and a contrast transfer function (CTF) are alternate ways to describe spatial resolution. In this work we measured the system LSF, then calculated the CTF by convolving the LSF with square waves of various frequencies. Images recorded with Ronchi ruling masks confirm the accuracy of the CTF calculation.

Figure 1(a) shows the LSF measured using a 18-ns laser pulse entering the camera through a 10- μm wide spatial mask. Spatial resolution referred to the photocathode is 40 μm [full width at half maximum (FWHM)]. The LSF is a sharp spike rising a factor of 400 above the noise. The slightly asymmetric shape has not been investigated and is likely an artifact of our measurement technique. The calculated CTF [Fig. 1(b)] shows a 60% contrast transfer ratio (CTR) at 10 lp/mm and a limiting visual resolution (5% CTR) > 20 lp/mm. CTR measurements with 6 and 10 lp/mm Ronchi rulings confirm the validity of the CTF calculation.

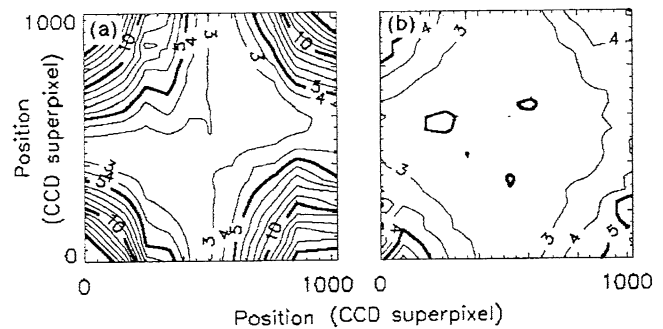


FIG. 2. Contour maps showing position dependence of camera spatial resolution. (a) 1-mm wide slit, (b) 100- μm slit. Contours labels are in 2×2 superpixels.

The contour plots in Fig. 2 show the position dependence of the spatial resolution for the entire streak camera image. Data were recorded using a mask with 10- μm openings every 1.5 mm. The FWHM is determined at various spatial positions throughout the image. Contour plots are presented for input slit widths of 1 mm and 100 μm . Improved spatial resolution is obtained with the narrow slit, but dynamic range is reduced by about 5. (For the P-510 tube, we found that only the central 500 μm of the 1 mm region illuminated by the laser actually contributes to the tube's signal).

Three factors influence time resolution: electron transit-time spread, dwell time and slit image width in the temporal direction. A simple static measurement in which the deflection plates are grounded and the tube illuminated with a dc light source provides an excellent estimate for camera temporal resolution. The FWHM Δx of the static line represents the best temporal resolution (in pixels) possible with the camera. To estimate temporal resolution, multiply Δx by the dwell time (ps/pixel) of the sweep obtained from a time base calibration and add in quadrature with the electron transit-time spread (typically 6 to 10 ps). For this camera temporal resolutions of 12, 22, and 45 ps FWHM are estimated for the 2.3, 5.3, and 11.2 ns sweep windows (nominally referred to as 2, 6, and 12 ns sweep windows). Resolution was checked for consistency by measuring the width of a short (45 ps FWHM) laser pulse at each sweep speed.

We generated an image in which a series of voltage steps were applied to the deflection plates. The resulting image is a set of constant time lines each of which can be analyzed along its spatial extent. Figure 3 shows a contour map of the

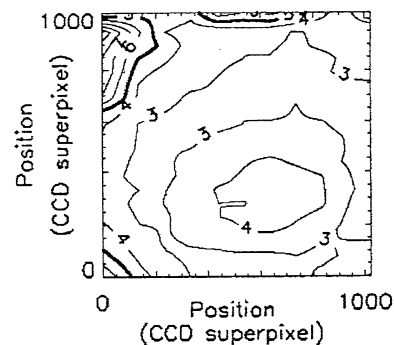


FIG. 3. Contour map showing position dependence of time resolution for 100- μm slit. Contours labels are in 2×2 superpixels.

position dependence of the temporal resolution (in pixels) in the streak camera image. With a 100- μm slit, 90% of the image has a resolution $<5 \times 2 \times 2$ superpixels (FWHM).

Dynamic range depends on camera noise and gain. Noise establishes the weakest signal that can be observed. Gain determines whether or not a single event can be seen. Background images contain information about read noise, dark current noise, and signal threshold. They verify the noise reported by the CCD manufacturer and determine if additional noise is introduced by the other streak camera components. For this work, we measured image noise for two-second exposures with different hardware binning configurations. For no binning we measured system noise of $5.13 e^-$, nearly identical to the CCD specification of $5.05 e^-$. This indicates that nearly all camera noise comes from the CCD. Dark current causes a slight increase in noise when pixels are binned for readout: 5.97, 6.67, and $7.9 e^-$, respectively, for 2×2 , 3×3 , and 4×4 binning.

Photocathode sensitivity tells how well the photocathode converts incident light to photoelectrons. The manufacturer measured this tube's sensitivity to be 25 mA/W at 532 nm. Gain describes how well each signal photoelectron is amplified and converted into CCD electrons. We measured system gain by illuminating a $3 \text{ mm} \times 0.5 \text{ mm}$ region of the photocathode with laser pulses of known energy and recording the images. The number of ADUs (analog-to-digital units) in a recorded signal divided by the incident energy gives the gain in ADUs/nJ. Using the photocathode sensitivity and the CCD gain (1.09 CCD e^- /ADU) allows conversion of this value to CCD electrons/photoelectron (CCD e^- /pe). For this camera we measured 101 CCD e^- /pe which agrees well with an independent gain measurement of 108 CCD e^- /pe.⁴

Maximum usable signal divided by the minimum observable signal defines dynamic range. For this work, dynamic range is determined per streak camera resolution element (32 pixels, i.e., four CCD pixels in space, and eight CCD pixels in time). We consider the maximum usable signal to be that at which the temporal pulse broadens by 20%. When the streak tube is the limiting element, temporal broadening is correlated with the Child-Langmuir (C-L) space-charge-limited current at the photocathode. A 20% broadening occurred at $\sim 1\%$ of the C-L current (Fig. 4). This corresponds to 500, 1150, and 2450 photoelectrons per streak camera resolution element at 2, 6, and 12 ns sweeps, respectively. (This is calculated using $0.01 \times J_0 \times \Delta A \times \Delta t \times N_{\text{pix}}/q$ where $J_0 = 2.2 \text{ A/cm}^2$, $\Delta A = 0.00005 \text{ cm}^2$ ($500 \times 10 \mu\text{m}$), Δt is the dwell time, $N_{\text{pix}} = 32$ pixels, and $q = 1.602 \times 10^{-19} \text{ C/e}$.)

We use signal-to-noise ratio (SNR) as a figure-of-merit to determine the minimum observable signal. Using $\text{SNR} = C/[(N_{\text{pix}}/N_b)\sigma_b^2]^{1/2}$, where C is the system gain to a single photoelectron in CCD electrons, N_{pix} is the number of detector pixels in a resolution element (32), N_b is the number of CCD pixels in a binned superpixel, and σ_b is the noise associated with reading a superpixel. SNR values are 3.5, 6, 8, and 9 for N_b of 1, 4, 9, and 16 (unbinned, 2×2 , 3×3 , and

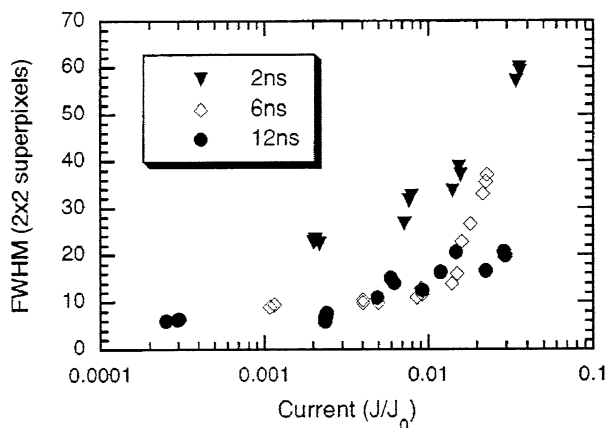


FIG. 4. Temporal broadening of 45-ps laser pulse versus streak tube current density for 2, 6, and 12 ns sweep speeds. $J_0 = 2.2 \text{ A/cm}^2$.

4×4), respectively. Superpixels of 2×2 allow detection of a single photoelectron ($\text{SNR} > 5$) with minimal degradation in data resolution. Thus, dynamic range for the 2, 6, and 12 ns sweep windows are 500, 1150, and 2450, respectively.

IV. DISCUSSION

The streak camera performs very well and appears to satisfy most NIF optical streak camera requirements. Magnification, FOV, temporal resolution, and sweep linearity are comparable to the current LLNL camera. The ROSS, however, excels in spatial resolution with a 40- μm (FWHM) LSF and $>20 \text{ lp/mm}$ CTR (limiting visual), about three times better than the LLNL camera's 120 μm (FWHM) and 9 lp/mm. By excluding the IIT from the ROSS design, the main resolution-broadening component has been eliminated. The P-510 tube with its FO coupled, back-thinned CCD produces enough gain that individual photoelectrons are observed and that dynamic range approaches the number of photoelectrons that can be linearly extracted from the photocathode in a streak camera resolution element.

ACKNOWLEDGMENTS

The authors thank the talented and creative LLE design team for their help fielding the prototype camera at Livermore. Wade Bittle, Mark Donovan, and Keith Ebbecke provided electrical engineering support; Gregory Antonini (of LLNL on assignment at LLE), Andrew Dillenbeck, and Lorie Hayes provided mechanical engineering support. This work was performed under the auspices of the U.S. Department of Energy by University of California Lawrence Livermore National Laboratory under Contract No. W-7405-ENG-48.

¹S. W. Thomas, J. W. Houghton, G. R. Tripp, and L. W. Coleman, *Proceedings of 11th International Congress on High Speed Photography*, edited by P. J. Rolls (Chapman and Hall, London, 1975), p. 101.

²W. R. Donaldson, R. Boni, R. L. Keck, and P. A. Jaanimagi, *Rev. Sci. Instrum.* **73**, 2606 (2002).

³J. D. Wiedwald and R. J. Hertel, *Proc. SPIE* **981**, 154 (1988).

⁴S. Ghosh, R. Boni, and P. A. Jaanimagi, *Rev. Sci. Instrum.*, these proceedings.